Condensation/evaporation coefficient and velocity distributions at liquid–vapor interface[1]

Takaharu Tsuruta*, Hiroyuki Tanaka, Takashi Masuoka

Department of Mechanical Engineering, Kyushu Institute of Technology, 1-1 Sensui-cho, Tobata-ku, Kitakyushu 804-8550, Japan

Abstract

Molecular dynamics simulations have been conducted for a system of argon molecules to study the effects of translational motion of monatomic molecules on condensation and evaporation coefficients. The results show that both coefficients depend on a surface-normal component of the translational energy. The vapor molecules with smaller energy can be easily reflected by the surface molecules, and the surface molecules with smaller energy can not evaporate. Also, velocity distributions of evaporated and reflected molecules are presented in the form of modified Maxwellian utilizing the condensation/evaporation coefficient expressed as a function of the normal component of translational energy. © 1999 Elsevier Science Ltd. All rights reserved.

1. Introduction

With progression of advanced technologies using evaporation and condensation, the interphase mass transfer between liquid and vapor phases has become very important in recent years from the viewpoints of molecular and microscale mass transfer. Following an ordinary approach to a description of interphase mass transfer rate, mass fluxes of vapor molecules crossing a plane immediately close to the liquid surface are expressed based on the kinetic theory of gasses. Net evaporation or condensation rate can be obtained from the difference between the fluxes of molecules moving outward from and toward the liquid surface.

Schrage [1] made a significant contribution to this problem and his theoretical expression for the interphase mass transfer rate was widely used at one time. Later Labuntsov [2,3] revised Schrage's expression by considering the non-equilibrium effects in the Knudsen layer adjacent to the liquid surface, and derived a modified expression for near-equilibrium condition. In addition to this, a number of studies, for example Sone and Onishi [4,5], Labuntsov and Kryukov [6] and Aoki et al. [7], conducted more elaborate studies to obtain approximate or numerical solutions of the Boltzmann equation for the non-equilibrium effects in the Knudsen layer.

In all of these theoretical studies, several assumptions have been made concerning the boundary conditions at the liquid surface. Condensation and evaporation coefficients are introduced to express the condensation probability (i.e. reflection rate) and the evaporation rate, respectively. In general, the condensation coefficient is defined as a fraction of incident molecules upon a liquid surface which remain in the liquid phase and the evaporation coefficient as the number ratio of emitted molecules from the liquid surface to those calculated by assuming a Maxwellian velocity distribution corresponding to a saturated vapor at the surface temperature. Since the two coefficients should coincide with each other under the thermal

---

* Corresponding author.
[1] The manuscript has not been simultaneously submitted for publication elsewhere.

Nomenclature

E_{in}	energy of an incident molecule	α_c	condensation coefficient
ΔE	energy change of reflected molecule	α_e	evaporation coefficient
F	velocity distribution function	β	parameter in Eq. (2)
k	Boltzmann constant	$\phi(r)$	potential function
m	mass of molecule	θ	incident angle of molecule on liquid surface
N	number of molecules		
r	distance of molecules		
T	temperature	*Subscripts*	
V	velocity	c	condensing surface
x, y, z	coordinates	in	inward direction from bulk
		out	outward direction from liquid surface
Greek symbols		x–y	of tangential component to liquid surface
α	parameter in Eq. (2)	z	of normal component to liquid surface

equilibrium condition, the same value is used even in the near-equilibrium state and represented by the term of condensation coefficient.

Since the condensation coefficient is an unknown important factor to express the interphase mass transfer rate, some experimental and theoretical efforts to obtain the reliable value are being continued. For liquid-metals such as mercury [8] and potassium [9], values close to unity have been obtained in the experiments of film condensation heat transfer. On the other hand, for polyatomic vapors such as water, methanol, carbontetrachloride and glycerol vapor, values less than unity have been reported in the experimental studies using a dropwise condensation method [10,11] and a shock-tube technique [12,13]. Also, a theoretical estimation of condensation coefficient have been developed by Fujikawa and Maerefat [14] on the basis of the transition state theory of statistical mechanics. The results are in good agreement with their experimental data for polyatomic vapors and they concluded that the condensation coefficient of polyatomic vapor is significantly smaller than unity because of a constraint of rotational motion of molecules in the liquid state. However, recent molecular dynamics studies have presented a different explanation for the small values of condensation coefficients of polyatomic vapors. Matsumoto et al. [15–18] carried out the molecular dynamics simulations for equilibrium vapor–liquid systems and obtained a good agreement with the experimental condensation coefficient by Fujikawa et al. [12,13]. They suggested that the condensation coefficients of polyatomic molecules are reduced due to molecular exchange like a spattering phenomena caused by collisions of vapor molecules with the liquid surface. This suggestion is very interesting but needs further investigation since their definition of conden-

sation coefficient seems to be different from the ordinary one.

Let us turn to the monatomic vapor. According to the transition state theory by Fujikawa and Maerefat [14], the condensation coefficients of monatomic vapors must be unity because they are free from the rotational motion. Here, it should be noted that there is no difference between the evaporation from the liquid surface and the diffusive outflow from the reservoir of the saturated vapor when the condensation coefficient has a value of unity. In this case, no consideration for effects of the liquid surface is included and the molecules evaporated from the liquid surface are treated as those having the same Maxwellian velocity distribution as the uniform vapor. Our molecular dynamics study [19] showed that the condensation probability of argon molecules is close to unity (over 0.9 at 84 K) but it decreases with surface-normal component of translational energy. This indicates a dependency of the condensation coefficient upon the translational motion of incident molecules. In the present study, therefore, focussing on the effect of translational motion, condensation and evaporation behaviors are studied in detail using the molecular dynamics method for an argon molecule system. The condensation coefficient is expressed as a function of translational energy and the surface temperature. Furthermore, the velocity distributions near the interface zone are analyzed and compared with the Maxwellian distribution. The evaporation coefficients are also presented as a function of translational energy of evaporated molecules.

2. Simulation method

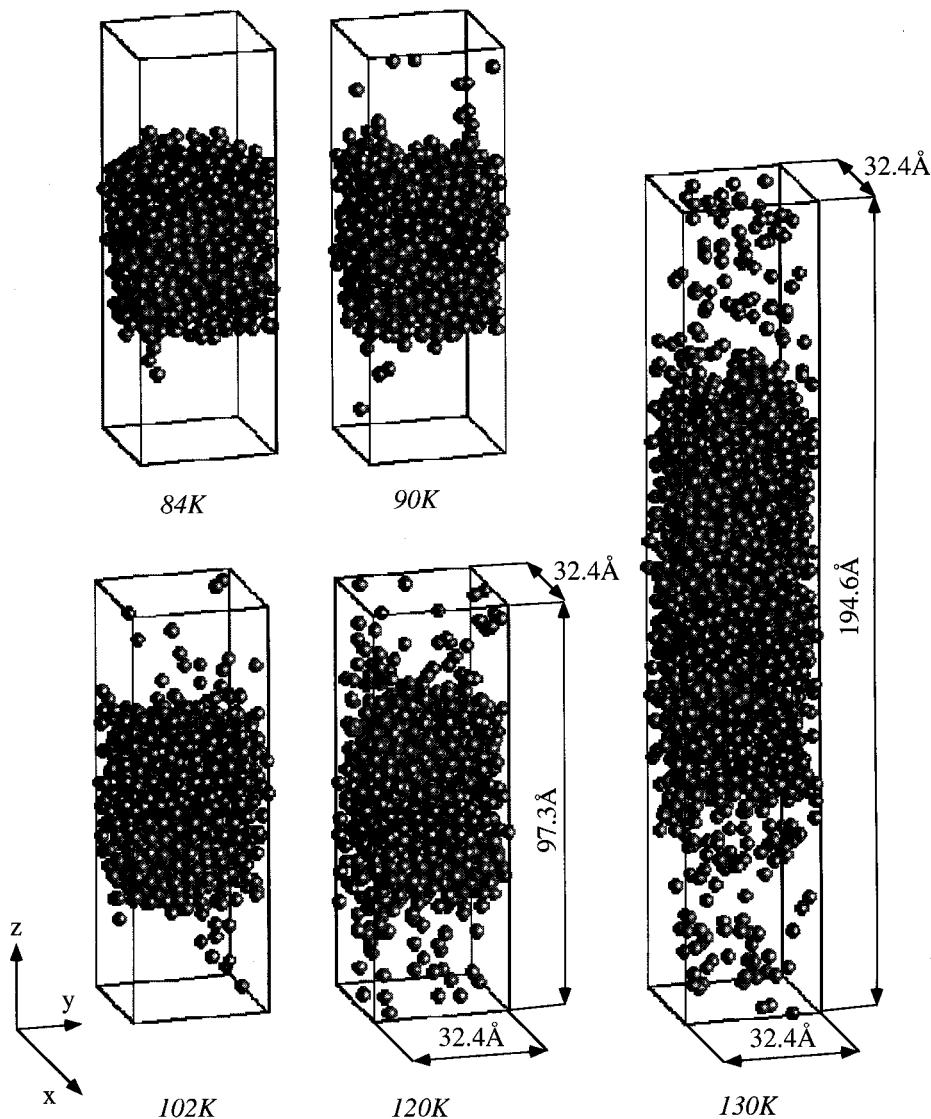By following our previous study [19], the molecular

Fig. 1. Snapshot of simulation system.

dynamics simulations for argon molecules have been performed for different system temperatures. To formulate the liquid–vapor interface, the simulation technique developed by Matsumoto and Kataoka [15] was employed. Fig. 1 shows 3-dimensional snapshots at five system temperatures of 84, 90, 102, 120 and 130 K in the simulation. The basic cell is a rectangular enclosure with the periodic boundary conditions for all boundaries. The number of molecules in the system is 864 for the temperatures of 84–120 K and 1728 for 130 K. Intermolecular potential is a simple Lennard–Jones 12–6 potential:

$$\phi(r) = 4\epsilon\{(\sigma/r)^{12} - (\sigma/r)^6\} \qquad (1)$$

which provides a reasonable description of the properties of many nonpolar molecules [20,21]. It must be emphasized here that the potential is not for an isolated pair of molecules since the parameters σ and ϵ are generally chosen so as to approximate the properties in the one-phase region [22]. Nevertheless, Eq. (1) has been used in the computer simulation for phase transitions and a comparison of the liquid–gas coexistence curve with the experiment has been presented in the case of argon [23]. Based on the comparison, Matsumoto and Kataoka [15] used the values of $\sigma = 3.405$ Å and $\epsilon/k = 119.8$ K for the interphase mass transfer problem and we also use the same values for simplicity. To integrate the Newton's equation of
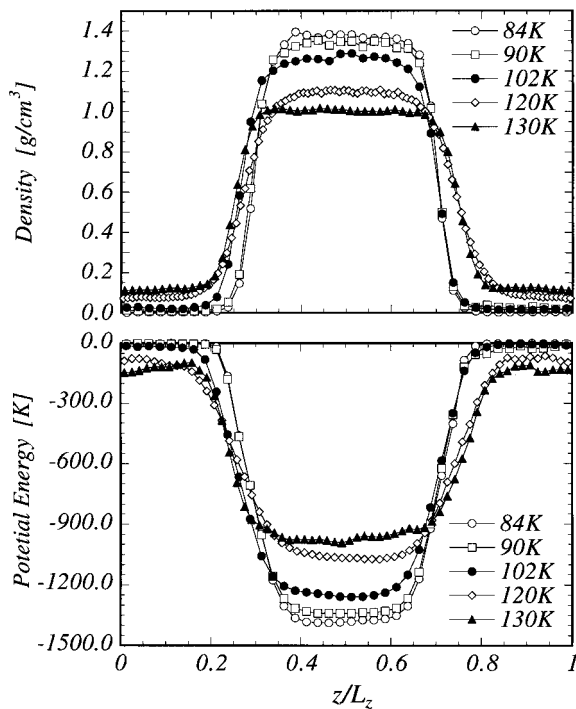
Fig. 2. Density and potential energy profiles.

motion, the Verlet method is used with the time step of 5.0 fs. The cutoff radius is 3.5 σ.

Density profiles calculated are shown in Fig. 2 together with potential energy profiles. These profiles mean time-averaged value during steady state period of 150 ps for 84 K-system or 200 ps for the others. Even in the steady state, the system temperature showed the fluctuation of ± 5 K. The densities at the central liquid region are around 1.35, 1.33, 1.25, 1.10 and 1.00 g/cm^3 in order of the system temperature, which are close to the reported values for the saturated liquid. We can see an interphase zone between the liquid and vapor phases where the changes in density and potential energy occur. The interphase zone is dealt with the liquid surface in this paper.

First in the present study, an argon molecule is injected as a test molecule with a different translational energy and an incident angle into the system in order to study how the condensation probability depends on the translational motion of a vapor molecule. For a set of translational energy and incident angle, 100 random injections are conducted to examine the condensation or reflection behaviors. The details of the incident method are described in Ref. [19]. The injection simulation is carried out for the systems of 84, 90 and 102 K.
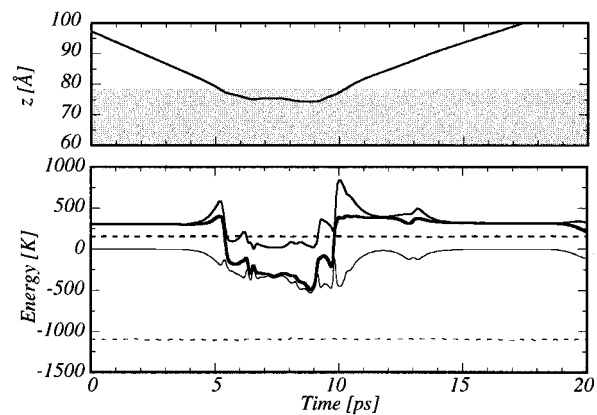
Next, velocity distributions of the evaporated and reflected molecules are measured at the vicinity of the
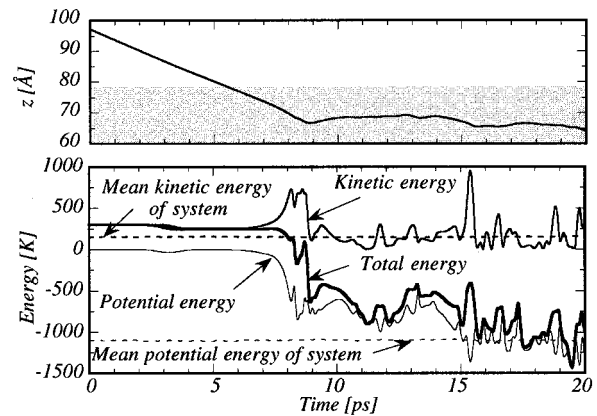
(a) Case of condensation
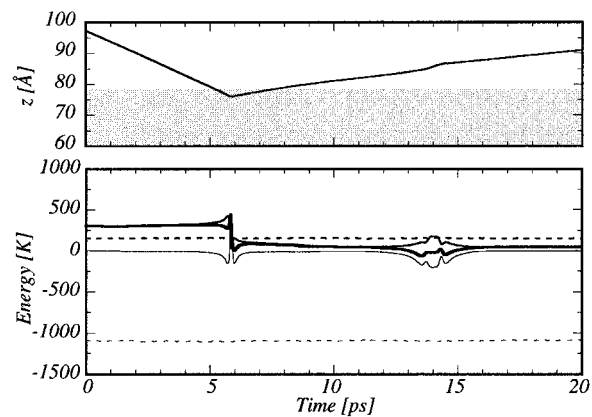
(b) Case of reflection at one collision

(c) Case of reflection due to several collisions

Fig. 3. Typical time histories of incident molecules in 102 K system (initial incident energy: $E_{in} = 300$ K, incident angle: $\theta = 0$ degree).

liquid surface and compared with the Maxwellian distribution. The measurements are made for a relatively long duration in the thermal equilibrium system at

102, 120 and 130 K. From the viewpoint that the evaporation coefficient should be equal to the condensation coefficient in the equilibrium state, the evaporation coefficient is examined and the relation between the evaporation coefficient and velocity distribution of evaporated molecules is discussed.

3. Surface-collision behaviors and condensation coefficient

3.1. Trajectories and energy histories of incident molecules

Typical trajectories and time histories of energies of incident test molecules are shown in Fig. 3 for the system at 102 K and we can see the typical process of condensation or reflection in these figures. The shaded regions correspond to the interphase zone in Fig. 2. Energy is represented in the unit of absolute temperature (divided by the Boltzmann constant k). Time at the collision between the test incident molecule and the surface molecules can be found from a steep change of potential energy.

In the case of Fig. 3(a) where the incident molecule is captured by the liquid phase, the molecule repeats the collisions several times within the interphase zone and loses its kinetic energy. Through some collisions the kinetic and potential energies approach to the mean values of the liquid-film system, then the process of phase transformation from the vapor to the liquid is completed. In the case of reflected molecules as shown in Fig. 3(b) and (c), on the other hand, we can see a small number of collisions. It is therefore understood that the collisions repeated in the interphase zone raise the probability of condensation. Our previous study [19] also indicated that the first collision occurring at the outer location of the interphase zone reduces the iterative collision due to the low density and increases the probability of reflection.

3.2. Condensation coefficient

The condensation coefficient is defined as the fraction of incident molecules which condense on the liquid surface. By counting the number of the condensed case in the injection simulation, the condensation coefficients are obtained for all incident conditions. The results are plotted in Fig. 4 as a function of normal component of initial incident energy $E_{in,z}$. The figure includes the data for the surfaces of 120 and 130 K obtained using a different method described later. Although the value of the condensation coefficient for the surface of 84 K is close to unity, we can see that the increase of surface temperature reduces the condensation coefficient. The decrease is
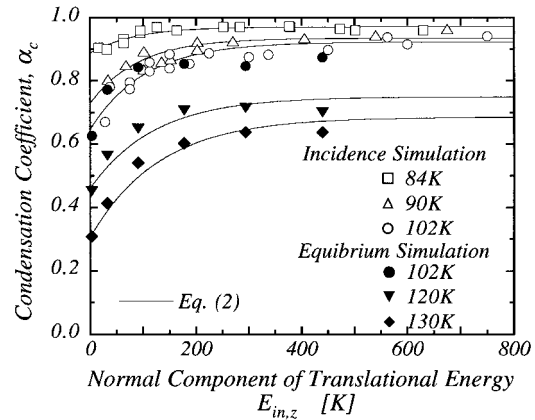

Fig. 4. Condensation coefficient as a function of translational energy.

significant for the smaller energy and the condensation coefficient increases with the energy. Judging from the collision behavior of molecules, this is because that the incident molecule is easily reflected if the surface molecules have a larger kinetic energy compared with the incident molecule. It is also considered that the vapor molecules with large kinetic energy can penetrate the interphase zone which enable them to repeat the collisions with the surface molecules and increase the condensation probability.

Based on the simulation results that the condensation coefficient increases with the normal component of translational energy and decreases with the increase of system temperature, regression curves expressed by the following formulation are applied for the condensation coefficient α_c:

$$\alpha_c = \alpha \left\{ 1 - \beta \, \exp\left(-\frac{E_{in,z}}{kT_c} \right) \right\} \tag{2}$$

where α and β are constants to be determined by the regression. The results are presented in Fig. 4 by the solid lines and they show good agreement with the results of the molecular dynamics simulation. The parameters α and β are shown in Table 1.

Table 1
Parameters of condensation coefficient in Eq. (2)

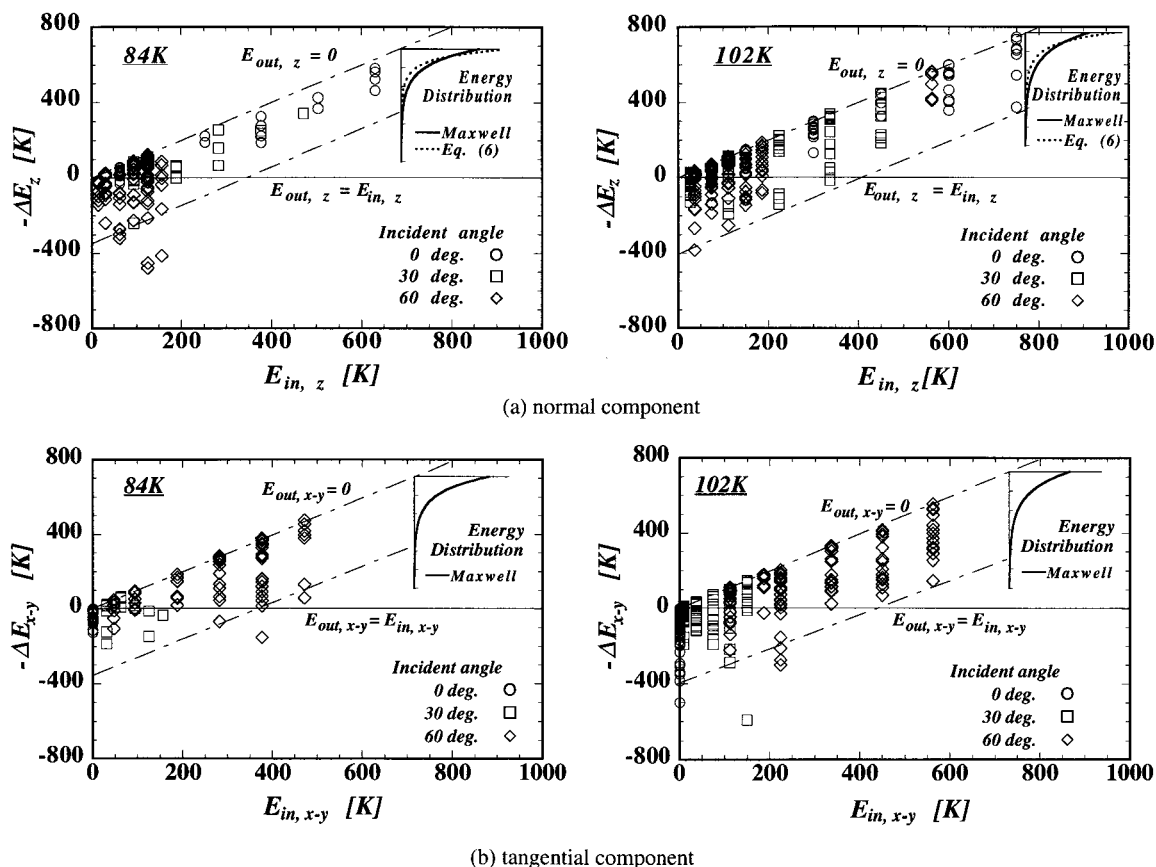| Temperature, T_c [K]	α	β
84	0.971	0.086
90	0.935	0.220
102	0.923	0.299
120	0.750	0.388
130	0.685	0.554

Fig. 5. Energy losses of reflected molecules at 84 and 102 K surfaces.

3.3. Energy change of reflected molecule

Information concerning the reflected molecules is also necessary as a boundary condition for the molecular kinetics in the vapor phase. Fig. 5 shows energy losses $-\Delta E$ of the reflected molecules in the simulations for 84 and 102 K; here the energy change ΔE is calculated as the energy difference between the energy E_{out} at the time when the reflected molecule goes out from the simulation cell and the initial incident energy E_{in}, i.e. $\Delta E = E_{out} - E_{in}$. The upper figures are for the surface-normal component ΔE_z and the lower figures for the tangential component ΔE_{x-y}. The negative values in Fig. 5 mean that the reflected molecules obtained the energy from the surface molecules. It is found in each figure that the molecules having the small incident energy gain the energy by the collisions with the surface molecules. The molecules with larger incident energy, on the other hand, lose most of their energy since they have a large possibility to repeat the collisions in the interphase zone. There is no tendency to conserve the energy ($E_{out} = E_{in}$) at the collisions. In each energy component, the energy losses are located between two diagonal lines. The upper line indicates an upper limit of energy loss, $E_{out} = 0$. The lower line is drawn by assuming the Maxwellian velocity distribution for the surface temperature, that is, the reflected molecules are assumed to be well accommodated to the liquid surface and scattered according to the Maxwellian. For this case, the distribution curves of the energy losses are presented in the figures. Although the number of data is limited because of the small reflection rate, the data seems to be well expressed by the energy distribution curves. Therefore, an accommodation coefficient for the energy of reflected molecules is considered to have a value of unity and this is supported from the results, as they repeat the collisions with the surface molecules. Strictly speaking as for the normal component of velocity distribution, the Maxwellian should be modified by utilizing the evaporation/condensation coefficient as shown in the next chapter. This modification was made for the energy distribution curves and expressed by dotted curves in Fig. 5(a). We can see little effect of the modification.
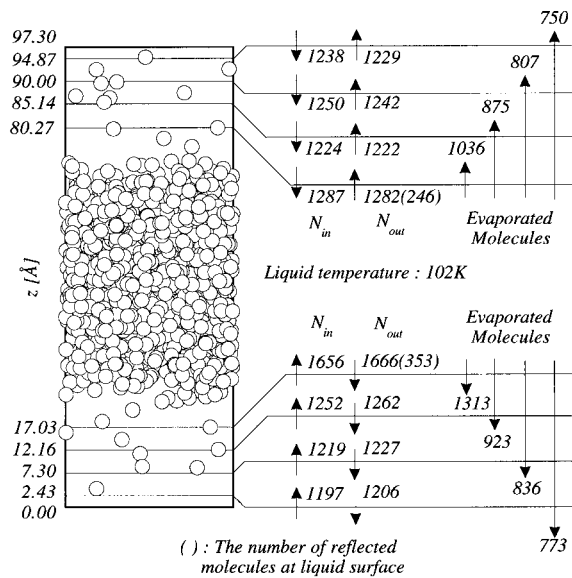
Fig. 6. Number of leaving and approaching molecules during 5000 ps in 102 K system.

(a) tangential component : Vx

(b) tangential component : Vy

(c) normal component : Vz

Fig. 7. Histograms of leaving molecules from $z = 17.03$ and 80.27 Å in 102 K system.

4. Velocity distributions and evaporation/condensation coefficient

4.1. Measurements of velocity distributions

Equilibrium simulations with evaporation and condensation have been carried out for the systems of 102, 120 and 130 K, in order to study the velocity distributions of evaporated and reflected molecules and their relations to the evaporation/condensation coefficient. The condensation coefficient and the evaporation coefficient should coincide with each other at the equilibrium state. The molecular dynamics simulations were carried out for another duration of 1200–5000 ps after formulating the equilibrium liquid-film system and molecules crossing several planes parallel to the surface were measured. Fig. 6 shows the numbers of molecules counted in the simulation of the 102 K system. N_{in} and N_{out} denote the numbers of crossing molecules inward from the bulk vapor and outward from the liquid surface, respectively. Since both numbers are almost equal in each z-location, it is confirmed that the system is in a thermal equilibrium state.

The number of evaporated molecules, which are emitted from the liquid phase, is estimated by subtracting the reflected molecules at the liquid surface from the molecules crossing away from the closer plane ($z = 17.03$ and 80.27 Å) to the liquid film. The number in parenthesis in Fig. 6 indicates the reflected molecules out of the incoming N_{in}. We can see the number of evaporated molecules decreases with distance from the liquid surface. The number of molecules are sum-
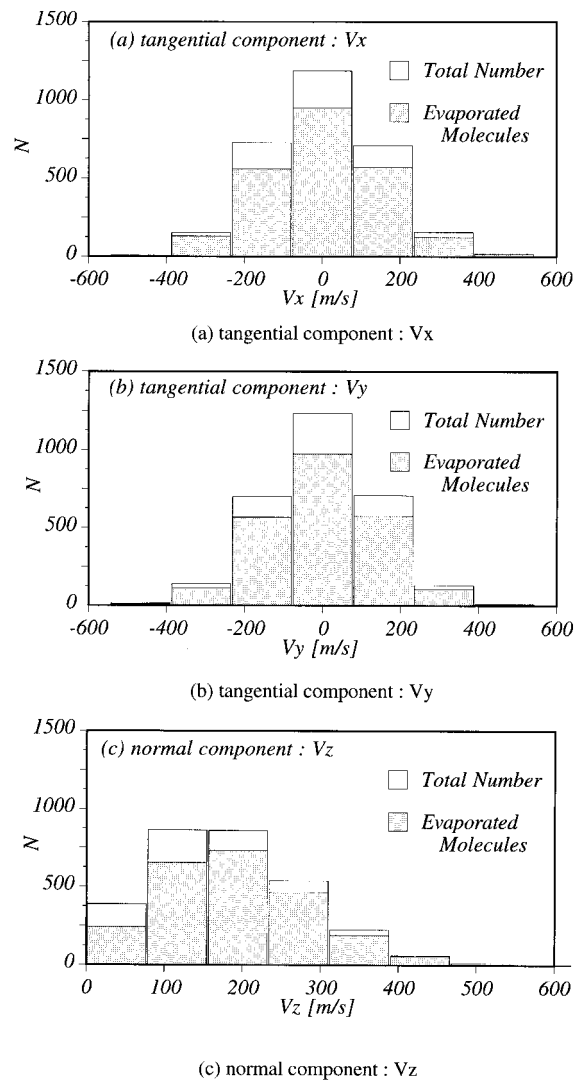
marized in the form of a histogram as shown in Fig. 7. Here, three components of velocity V_x, V_y, V_z are considered separately and the evaporated molecules are depicted by shadings in the histogram. It is understood that the leaving molecules consist of evaporated and reflected molecules and we can estimate the ratio of evaporated molecules to the leaving molecules in each velocity range. From the ratio, the evaporation coefficient will be obtained as a function of velocity in the next section.

Fig. 8 shows the velocity distribution functions of all leaving, evaporated and reflected, molecules for a comparison with the Maxwellian velocity distribution given by the following forms:
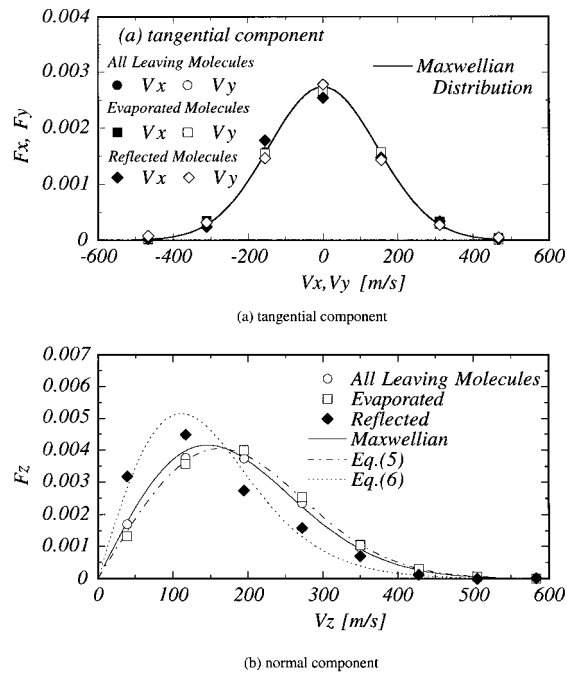
(a) tangential component

(b) normal component

Fig. 8. Velocity distributions of leaving molecules from the liquid surface at 102 K.

$$F_i = \left(\frac{m}{2\pi k T_c}\right)^{1/2} \exp\left(-\frac{mV_i^2}{2kT_c}\right) \quad (i = x \text{ or } y) \qquad (3)$$

$$F_z = \left(\frac{m}{kT_c}\right)V_z \exp\left(-\frac{mV_z^2}{2kT_c}\right) \qquad (4)$$

For the tangential components of velocity V_x and V_y in Fig. 8 (a), all distribution functions are consistent with the Maxwellian and there is no marked difference between three kinds of molecules (all leaving, evaporated and reflected molecules). For the normal component V_z, however, we can find some systematic differences in the velocity distributions. Although the velocity distribution for all leaving molecules is well expressed by the Maxwellian distribution, the evaporated and reflected molecules show different distributions. The distribution function for the evaporated molecules is larger than the Maxwellian in the large velocity region but is smaller in the low velocity region. On the contrary, the reflected molecules show a higher distribution density than the Maxwellian in the low velocity region and a smaller density in the large velocity region. In other words, most leaving molecules with the large normal component of velocity are the evaporated molecules, but those leaving molecules with smaller velocity are reflected molecules. The results presented here are for the 102 K system; however, this study has included the 120 and 130 K systems and
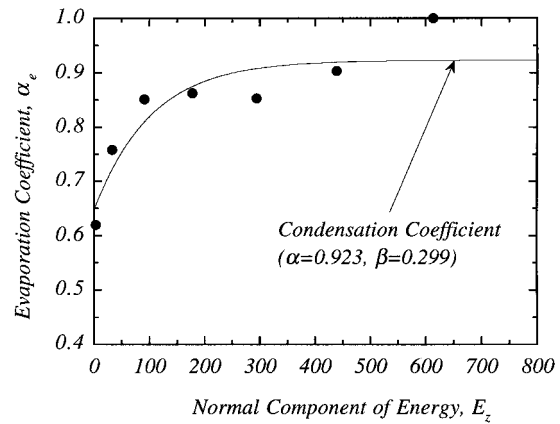

Fig. 9. Comparison of evaporation coefficient with condensation coefficient.

their results are qualitatively the same. Since these systematic characteristics on the evaporated and reflected molecules should be considered in the kinetic theory for the interphase mass transfer, the expressions of the velocity distributions will be shown by introducing the evaporation coefficient defined as a function of velocity.

4.2. The evaporation coefficient and velocity distribution functions

Evaporation coefficient has been used to compensate the difference between the molecular flux due to real evaporation and the predicted flux based on the kinetic theory assuming the Maxwellian. If the evaporation coefficient has a value of unity, therefore, all leaving molecules are the evaporated and their velocity distribution is given by the Maxwellian velocity distribution. In accordance with the definition of the evaporation coefficient, the fraction of evaporated molecules to all leaving molecules is obtained in each velocity region. Typical results are plotted in Fig. 9 as a function of the normal component of translational energy, which is obtained from the histogram presented in Fig. 7 for the system of 102 K. The evaporation coefficient increases with the normal component of the translational energy in a similar way to the condensation coefficient. The dependency of the evaporation coefficient on the normal component of translational energy indicates that the molecules having a large normal component of kinetic energy can easily escape from the influence of the liquid surface, while it is difficult for molecules with smaller energy.

The evaporation coefficient has the same value as the condensation coefficient under the thermal equilibrium condition. From this viewpoint, the results on the evaporation coefficient in the 102 K system are

compared in Fig. 9 with Eq. (2) for the condensation coefficient obtained in the injection simulations. The solid line is the condensation coefficient. We can see a good agreement between them, while some differences are seen in the higher energy regions. The reason for the discrepancy is understood from Fig. 7: that the number of molecules in the higher energy region was not enough to compare with the results from the injection simulation. However, in the other region there is no marked difference between them because there are enough samples. By considering the limitation of sample number, the condensation coefficient, Eq. (2) with $\alpha = 0.923$ and $\beta = 0.299$, is recommended as the evaporation coefficient for the 102 K system. The condensation coefficients in Fig. 4 for the system temperature of 120 and 130 K are the evaporation coefficients obtained from the measurement of velocity distributions at the equilibrium state. In these higher temperature cases, evaporation and condensation become more active, so we get enough molecules to evaluate the evaporation coefficient.

Finally, relations between the condensation/evaporation coefficient and the velocity distribution functions of evaporated and reflected molecules will be discussed. By utilizing the condensation/evaporation coefficient in the form of Eq. (2) and by considering the definition that the evaporation coefficient is the ratio of evaporated molecules to the molecules estimated by the Maxwellian, we obtain the following velocity distribution functions for the evaporated and reflected molecules, respectively:

$$F_{z,e} = \frac{1 - \beta \, \exp(-mV_z^2/(2kT))}{1 - \beta/2} \left(\frac{m}{kT_c} \right) V_z$$
$$\exp\left(-\frac{mV_z^2}{2kT_c} \right) \tag{5}$$

$$F_{z,r} = \frac{1 - \alpha + \alpha\beta \, \exp(-mV_z^2/(2kT_c))}{1 - \alpha + \alpha\beta/2} \left(\frac{m}{kT_c} \right) V_z$$
$$\exp\left(-\frac{mV_z^2}{2kT_c} \right) \tag{6}$$

Here, the Maxwellian velocity distribution was modified by α_c for evaporated and $(1-\alpha_c)$ for reflected molecules, and the normalization procedures were performed to be the probability density functions.

Fig. 8(b) includes these distribution functions for the case of 102 K system with parameters $\alpha = 0.923$ and $\beta = 0.299$, and the comparison shows that these equations can express the behavior of evaporation and reflection at the liquid surface. The expressions of Eqs. (5) and (6) and the condensation/evaporation coefficient of Eq. (2) are considered to be important and useful as the boundary conditions for the kinetics of interphase mass transfer since they include the effects of molecular motion on condensation, evaporation and reflection.

5. Conclusion

The condensation and evaporation behaviors at the liquid-vapor interphase have been studied using the molecular dynamics method for the argon molecule system. The effects of translational motion on the condensation and evaporation coefficients were investigated to obtain the boundary conditions for the interphase mass transfer rate. The following conclusions have been derived:

1. The condensation/evaporation coefficient of monatomic molecules depends on their surface-normal component of translational energy. The vapor molecules with smaller incident energy are easily reflected by the surface molecules and the surface molecules with smaller energy cannot escape from the liquid surface. At elevated surface temperatures, the condensation/evaporation coefficient decreases due to the increasing ability of reflection by the surface molecules. The expression for the condensation/evaporation was presented as a function of the normal component of translational energy and the surface temperature.
2. All leaving molecules outward from the liquid phase which consist of evaporated and reflected molecules, show the Maxwellian velocity distribution under the thermal equilibrium condition. But the velocity distributions of the evaporated and reflected molecules deviate from the Maxwellian in the normal component of their velocity. The deviations are closely related to the dependency of the condensation/evaporation coefficient on the translational motion of molecules, and we obtained the velocity distribution functions for the evaporated and reflected molecules by modifying the Maxwellian with the use of the condensation/evaporation coefficient.

References

[1] R.W. Schrage, A Theoretical Study of Interphase Mass Transfer, Columbia University Press, New York, 1953.

[2] D.A. Labuntsov, An analysis of evaporation and condensation processes, Teplofisika Visokikh Temperature 5 (1967) 647–654.

[3] D.A. Labuntsov, An analysis of intensive evaporation and condensation, High Temperature (English Transl.) 5 (1967) 579–647.

[4] Y. Sone, Y. Onishi, Kinetic theory of evaporation and condensation, Journal of the Physical Society of Japan 35 (1973) 1773–1776.

[5] Y. Sone, Y. Onishi, Kinetic theory of evaporation and condensation—hydrodynamic equation and slip boundary condition, Journal of the Physical Society of Japan 44 (1978) 1981–1994.

[6] D.A. Labuntsov, A.P. Krykov, An analysis of intensive evaporation and condensation, International Journal of Heat and Mass Transfer 22 (1979) 989–1002.

[7] K. Aoki, Y. Sone, T. Yamada, Numerical analysis of gas flows condensing on its plane condensed phase on the basis of kinetic theory, Physics of Fluids A2 (1990) 1867–1877.

[8] J. Niknejad, J.W. Rose, Interphase matter transfer: an experimental study on condensation of mercury, Proceedings of the Royal Society of London A378 (1981) 305–327.

[9] R. Ishiguro, K. Sugiyama, An experimental study on intensive condensation of potassium, in: Proceedings of the Eighth International Heat Transfer Conference, 1986, vol. 4, pp. 1635–1640.

[10] H. Tanaka, S. Hatamiya, Drop size distributions and heat transfer in dropwise condensation—condensation coefficient of water at low pressures, in: Proceedings of the Eighth International Heat Transfer Conference, 1986, vol. 4, pp. 1671–1676.

[11] T. Tsuruta, T. Masuoka, Y. Kato, Estimation of condensation coefficient from dropwise condensation heat transfer, Thermal Science and Engineering 2 (1994) 98–103.

[12] S. Fujikawa, M. Okuda, T. Akamatsu, T. Goto, Non-equilibrium vapor condensation on a shock-tube end-wall behind a reflected shock wave, Journal of Fluid Mechanics 183 (1987) 293–324.

[13] M. Maerefat, S. Fujikawa, T. Akamatsu, T. Mizutani, An experimental study of non-equilibrium vapor condensation in a shock-tube, Experiments in Fluids 7 (1989) 513–520.

[14] S. Fujikawa, M. Maerefat, A study of the molecular mechanism of vapor condensation, JSME International Journal, Series II 33 (1990) 634–641.

[15] M. Matsumoto, Y. Kataoka, Study on liquid–vapor interface of water, I: simulational results of thermodynamic properties and orientational structure, Journal of Chemical Physics 88 (1988) 3233–3245.

[16] M. Matsumoto, Y. Kataoka, Molecular orientation near liquid–vapor interface of methanol: simulational study, Journal of Chemical Physics 90 (1989) 2398–2407.

[17] M. Matsumoto, K. Yasuoka, Y. Kataoka, Microscopic features of evaporation and condensation at liquid surface: molecular dynamics simulation, Thermal Science and Engineering 2 (1994) 64–69.

[18] M. Matsumoto, K. Yasuoka, Y. Kataoka, Molecular mechanism of evaporation and condensation, Thermal Science and Engineering 3 (1995) 27–31.

[19] T. Tsuruta, N. Sakamoto, T. Masuoka, Condensation process at liquid–vapor interface and condensation coefficient, Thermal Science and Engineering 3 (1995) 85–90.

[20] A.E. Sherwood, J.M. Prausnitz, Intermolecular potential functions and the second and third virial coefficients, The Journal of Chemical Physics 41 (1964) 429–437.

[21] A.A. Clifford, P. Gray, N. Platts, Lennard–Jones 12–6 parameters for ten small molecules, Journal of the Chemical Society: Faraday Transactions I 73 (1977) 381–382.

[22] M.P. Allen, D.J. Tildesley, in: Computer Simulation of Liquids, Oxford University Press, Oxford, 1987, pp. 7–9.

[23] J.-P. Hansen, L. Verlet, Phase transitions of the Lennard–Jones system, Physical Review 184 (1969) 151–161.